agriculture

MDPI

Article

OTUD7A Regulates Inflammation- and Immune-Related Gene Expression in Goose Fatty Liver

Minmeng Zhao [1], Kang Wen [1], Xiang Fan [1], Qingyun Sun [1], Diego Jauregui [1], Mawahib K. Khogali [1], Long Liu [1], Tuoyu Geng [1,2] and Daoqing Gong [1,2,*]

[1] College of Animal Science and Technology, Yangzhou University, Yangzhou 225009, China; mmzhao@yzu.edu.cn (M.Z.); dx120190116@yzu.edu.cn (K.W.); mx120190650@yzu.edu.cn (X.F.); mx120200832@yzu.edu.cn (Q.S.); dh18051@yzu.edu.cn (D.J.); dh16013@yzu.edu.cn (M.K.K.); 005978@yzu.edu.cn (L.L.); tygeng@yzu.edu.cn (T.G.)

[2] Joint International Research Laboratory of Agriculture and Agri-Product Safety of the Ministry of Education of China, Yangzhou University, Yangzhou 225009, China

* Correspondence: dqgong@yzu.edu.cn; Tel.: +86-138-0527-5847

Abstract: OTU deubiquitinase 7A (*OTUD7A*) can suppress inflammation signaling pathways, but it is unclear whether the gene can inhibit inflammation in goose fatty liver. In order to investigate the functions of *OTUD7A* and identify the genes and pathways subjected to the regulation of OTUD7A in the formation of goose fatty liver, we conducted transcriptomic analysis of cells, which revealed several genes related to inflammation and immunity that were significantly differentially expressed after *OTUD7A* overexpression. Moreover, the expression of interferon-induced protein with tetratricopeptide repeats 5 (*IFIT5*), tumor necrosis factor ligand superfamily member 8 (*TNFSF8*), sterile alpha motif domain-containing protein 9 (*SAMD9*), radical *S*-adenosyl methionine domain-containing protein 2 (*RSAD2*), interferon-induced GTP-binding protein Mx1 (*MX1*), and interferon-induced guanylate binding protein 1-like (*GBP1*) was inhibited by *OTUD7A* overexpression but induced by *OTUD7A* knockdown with small interfering RNA in goose hepatocytes. Furthermore, the mRNA expression of *IFIT5*, *TNFSF8*, *SAMD9*, *RSAD2*, *MX1*, and *GBP1* was downregulated, whereas *OTUD7A* expression was upregulated in goose fatty liver after 12 days of overfeeding. In contrast, the expression patterns of these genes showed nearly the opposite trend after 24 days of overfeeding. Taken together, these findings indicate that *OTUD7A* regulates the expression of inflammation- and immune-related genes in the development of goose fatty liver.

Keywords: *OTUD7A*; goose; inflammation; immune; nonalcoholic fatty liver disease

Citation: Zhao, M.; Wen, K.; Fan, X.; Sun, Q.; Jauregui, D.; K. Khogali, M.; Liu, L.; Geng, T.; Gong, D. *OTUD7A* Regulates Inflammation- and Immune-Related Gene Expression in Goose Fatty Liver. *Agriculture* **2022**, *12*, 105. https://doi.org/10.3390/agriculture12010105

Academic Editors: Heather Burrow and Michael Goddard

Received: 28 November 2021
Accepted: 11 January 2022
Published: 13 January 2022

1. Introduction

Some fish and birds are able to pre-deposit large amounts of fat in the liver for use during migration, and then the liver can return to its normal state without any obvious pathological symptoms. Geese, as the offspring of migratory birds, also have this characteristic. In agricultural production, this ability of geese is often used for fatty liver production. As a well-known liver-producing species, the fatty liver (typically composed of approximately 60% fat) of Landes geese can reach an 8–10-fold higher weight than the normal liver in a short period through overfeeding [1]. The changes that occur in goose fatty liver are physiological, with no overt injury or pathological symptoms [2,3]. Recent work indicates that the pro-inflammatory factor is suppressed in goose fatty liver vs. normal liver [4]. However, nonalcoholic fatty liver disease (NAFLD) in humans and mammals is frequently accompanied by inflammation [5,6]. Human NAFLD is prone to developing from simple steatosis to nonalcoholic steatohepatitis (NASH), cirrhosis, and even liver cancer, posing a serious threat to human health [7]. In addition, the incidence of fatty liver in livestock and poultry has also increased due to improved feed nutrition levels, reduced animal activity, and increased environmental stress in modern intensive livestock production, thereby

bringing economic losses to livestock production [8]. The differences between geese and other animals suggest that the goose liver utilizes a protection mechanism, although the underlying mechanisms remain unclear. Studies of this mechanism may provide information for developing approaches for preventing or treating NAFLD-associated complications in humans and economically important animals.

A previous study demonstrated that inflammation is important in the progression from simple steatosis to NASH [9]. The hepatic inflammatory response plays an important role in insulin resistance, oxidative stress, and endoplasmic reticulum stress. Inflammation can interact with insulin resistance, and inflammatory factors can interfere with insulin signaling pathways and deepen the degree of insulin resistance, leading to a further decrease in insulin sensitivity in liver cells. On the other hand, inflammation causes the activation of Kupffer cells and stellate cells in the liver, and induces the development of liver fibrosis and cirrhosis [10]. Therefore, inflammation has been widely studied as a possible target for NASH therapy. The nuclear factor κB (NF-κB) signaling pathway is activated in human and animal NAFLD models, and the pathway is a key pro-inflammatory signaling pathway leading to the progression of NAFLD to NASH [5,6]. Inhibition of the NF-κB pathway has been reported to reduce the expression of inflammatory factors in the liver and alleviate the progression of NAFLD [11].

The results of our preliminary transcriptomic analysis showed that a number of deubiquitinating enzymes, including ovarian tumor deubiquitinase 7A (*OTUD7A*), were significantly altered at the transcriptional level in the livers of overfed geese compared to controls, suggesting that deubiquitinating modifications are involved in the formation of fatty liver in geese. *OTUD7A*, also known as cellular zinc-finger anti-NF-κB 2, is a member of the ovarian tumor deubiquitinase family [12,13]. OTUD7A promotes deubiquitination of its target proteins, including tumor necrosis factor receptor-associated factor 6 (TRAF6) [13], thus suppressing the NF-κB signaling pathway. Thus, we speculated that *OTUD7A* could inhibit inflammation. However, the functions of *OTUD7A* in the development of NAFLD are unclear. Therefore, we investigated the function of *OTUD7A*, and identified genes and pathways involved in regulating *OTUD7A*, using goose fatty liver as a model.

2. Materials and Methods

2.1. Animal Experiment

Thirty-two healthy 63-day-old male Landes geese were selected and randomly assigned to a control group and an overfeeding group (16 geese per group). Geese in the control group were provided water and feed ad libitum, whereas the geese in the overfeeding treatment were overfed using previously described procedures and diets [14]. In brief, geese in the overfeeding group were subjected to 1 week of pre-overfeeding, followed by 24 days of overfeeding. During the period of pre-overfeeding, the feed intake was gradually increased from 100 g to 300 g per day. For formal overfeeding, the daily feed intake was 500 g for three meals per day in the first 5 days, followed by 1200 g for 5 meals per day in the remaining time. The feed used in this study was cooked maize (maize boiled for 5 min) supplemented with 1% plant oil and 1% salt. All geese were raised in cages. At 81 and 93 days of age, six geese per treatment were randomly selected and fasted overnight with free access to water; in the next morning (at 82 and 94 days of age), the geese were weighed and killed with an electrolethaler. After the geese were exsanguinated, the liver samples were collected and stored at −80 °C. All animal protocols were approved by the Institutional Animal Ethics Committee of Yangzhou University, with permission number 202103309.

2.2. Preparation of Goose Primary Hepatocytes

Hepatocytes were isolated from Landes goose embryos after 23 days of incubation [2]. Specifically, the goose embryo was removed from the egg and placed in a pre-sterilized tray. The abdominal quills were gently removed and the embryo was sterilized with 75% alcohol. The liver was quickly harvested, immersed in PBS, and rinsed 2–3 times. The chopped liver

was transferred to a Petri dish and digested with 0.1% type IV collagenase (Worthington Biochemical Corporation, Lakewood, NJ, USA) at 37 °C for 25 min. Subsequently, an equal volume of pre-warmed complete medium that consisted of Dulbecco's modified Eagle's medium (DMEM Gibco, Grand Island, NY, USA), 0.02 mL/L epidermal growth factor (PeproTech, London, UK), 100 IU/mL penicillin (Sigma-Aldrich, St. Louis, MO, USA), 10% fetal bovine serum (Gibco, USA), and 100 mg/mL streptomycin (Sigma-Aldrich, St. Louis, MO, USA) was added to terminate the digestion. The hepatocyte suspension was obtained by filtering through a 220-mesh sterile nylon mesh to remove large tissue clumps and cell clusters. After treating the cells with erythrocyte lysate (Solarbio Co., Ltd., Beijing, China), complete medium was added to the hepatocytes to form a new hepatocyte suspension. The cells were inoculated into 12-well plates at a density of 1×10^6/well and transferred to a 37 °C incubator with 5% CO_2. The medium was renewed after the first 6 h of incubation, and then every 24 h during subsequent incubation.

2.3. Overexpression of Goose OTUD7A

The pcDNA3.1(+) vector containing the goose *OTUD7A* coding sequence (CDS) and the empty vector were designed, isolated, and purified from Shanghai GenePharma Co., Ltd. (Shanghai, China). The CDS of *OTUD7A* was found to be 2808 base pairs. The *OTUD7A* sequence fragment was obtained by PCR; the fragment was digested separately using enzymatic digestion from the pcDNA3.1 vector, and the product was purified and ligated. The ligated products were transformed into bacterial receptor cells, and the clones grown were first identified by enzymatic cleavage to demonstrate that the target gene had been connected to the target vector. The positive clones were then sequenced and analyzed for comparison, and those that were correct were considered to be successful. The recombinant vector was extracted via ultrapure extraction to obtain the pcDNA3.1-*OTUD7A* vector. Goose primary hepatocytes that were transformed with empty vectors were taken as controls (control treatment), and the *OTUD7A* CDS vector was used for overexpression. The vectors were transfected using Lipofectamine 2000 (Biosharp, Hefei, China) according to the instructions of the manufacturer. Six replicates were used for each treatment. After 6 h of transfection, the culture medium was changed from Opti-MEM (Thermo Fisher Scientific, Waltham, MA, USA) to complete medium. Cells were harvested after 24 h of culture.

2.4. Transcriptome Analysis

The samples of the control treatment and *OTUD7A* overexpression were subjected to RNA sequencing analysis. Briefly, mRNA was purified from total RNA using poly-T oligo-attached magnetic beads (Sigma-Aldrich, St. Louis, MO, USA), after which fragmentation was performed. RNA degradation and contamination were monitored on 1% agarose gels. The RNA purity was checked using a spectrophotometer (IMPLEN, Westlake Village, CA, USA), and the integrity was assessed using the RNA Nano 6000 Assay Kit of the Bioanalyzer 2100 system (Agilent Technologies, Santa Clara, CA, USA). A total of 1 μg of RNA per sample was used as input material for cDNA library preparation. The libraries were generated using the NEBNext® Ultra™ RNA Library Prep Kit for Illumina® (NEB, Ipswich, MA, USA), following the manufacturer's recommendations. After library construction, initial quantification was carried out using a Qubit 2.0 Fluorometer (Thermo Fisher Scientific, Waltham, MA, USA). The insert size of the library was then measured using an 2100 Bioanalyzer (Agilent Technologies, Santa Clara, CA, USA). When the insert size met expectations, real-time quantitative PCR (RT-qPCR) was performed to accurately quantify the effective library concentration (effective library concentration should be higher than 2 ng/μL) in order to ensure library quality. Eight cell lanes were used for each cDNA library.

The clustering of the index-coded samples was performed on a cBot Cluster Generation System using the TruSeq PE Cluster Kit v3-cBot-HS (Illumina), according to the manufacturer's instructions. After cluster generation, the library preparations were se-

quenced on an Illumina NovaSeq platform (San Diego, CA, USA) using four fluorescently labelled dNTP, DNA polymerase, and splice primers, and 150 bp paired-end reads were generated. Raw data (raw reads) of FASTQ format were firstly processed through in-house Perl scripts. In this step, clean data (clean reads) were obtained by removing reads containing adapters, reads containing poly-N, and low-quality reads from raw data. The average clean base (clean reads × 150 bp) was 8.19 G. At the same time, the Q20, Q30, and GC content of the clean data were calculated. All of the downstream analyses were based on the clean data, with high quality; the reference genome was Anser cygnoides domesticus (assembly AnsCyg_PRJNA183603_v1.0, https://www.ncbi.nlm.nih.gov/genome/?term=Anser+cygnoides+domesticus, accessed on 28 November 2021). The reads per kilobase million (FPKM) of each gene were calculated based on the length of the gene and the reads count mapped to the gene. Differential expression analysis of two groups was performed using the DESeq2 R package (Bioconductor, version 1.16.1, http://www.bioconductor.org/about/, accessed on 28 November 2021). The resulting *p*-values were adjusted using the Benjamini–Hochberg approach for controlling the false discovery rate. The differentially expressed genes (DEGs) were defined as genes with a fold change of treatment over control >2 or <0.5, and *p*-value < 0.05. In addition, the clusterProfiler R package (Bioconductor, version 3.4.4, http://www.bioconductor.org/about/, accessed on 28 November 2021) was used to test the statistical enrichment of differential expression genes in Kyoto Encyclopedia of Genes and Genomes (KEGG) pathways.

2.5. RNA Interference Assay

The small interfering RNA (siRNA) was designed to target the goose *OTUD7A* CDS, and was generated by Shanghai GenePharma Co., Ltd. (Shanghai, China). The siRNAs were separately transfected into the primary hepatocytes (prepared as described in Section 3.2), and cultured in serum-free and antibiotic-free Opti-MEM (Thermo Fisher Scientific, Waltham, MA, USA) using Lipofectamine 2000 (Biosharp). Briefly, 5 μL of Lipofectamine 2000 was added to 95 μL of Opti-MEM and incubated at room temperature for 5 min to prepare solution A, whereas 5 μL of siRNA or negative control was added to 95 μL of Opti-MEM to prepare solution B. Subsequently, 200 μL of the liquid was added to each well after solutions A and B were mixed and incubated at room temperature for 23 min. The Opti-MEM was replaced with complete culture medium after transfection, and the transfection time was 6 h. The siRNA dose was 100 nM. Scrambled siRNA was taken as a negative control. Six replicates were used for the negative control and RNA interference groups. The best siRNA was selected based on its ability to suppress *OTUD7A* expression (Supplementary Figure S2). After evaluation, the sense strand sequence of the chosen siRNA was 5′-GCGUGUACAGUGAAGAUUUTT-3′, while the antisense strand sequence was 5′-AAAUCUUCACUGUACACGCTT-3′.

2.6. Gene Expression Analysis

Total RNA from liver samples and primary hepatocytes that were transformed with an empty vector or *OTUD7A* CDS vector, or with scrambled siRNA or siRNA targeting *OTUD7A*, was obtained using TRIzol reagent (TaKaRa Biotechnology, Shiga, Japan). The quality and quantity of mRNA were assessed using a NanoDrop 1000 spectrophotometer (Thermo Scientific, Wilmington, DE, USA). A total of 600 ng of RNA per sample was reverse-transcribed into cDNA using PrimeScript RT Master Mix kits (TaKaRa Biotechnology, Shiga, Japan). Real-time PCR was performed using an ABI 7500 real-time quantitative PCR (RT-qPCR) system (Applied Biosystems, Foster City, CA, USA) using SYBR® Premix Ex Taq™ kits (Takara Biotechnology Co., Ltd., Dalian, China). The reactions were as follows: 95 °C for 30 s, followed by 40 cycles of 95 °C for 5 s and 60 °C for 30 s, then 95 °C for 15 s, 60 °C for 60 s, and 95 °C for 15 s. Two technical replicates were made for each sample. The primers used are listed in Table 1. Relative quantification methods were used, and glyceraldehyde-3-phosphate dehydrogenase (*GAPDH*) was chosen as the reference gene. The fold change level of mRNA was analyzed using the $2^{-\Delta\Delta CT}$ method [15].

Table 1. Primer sequences for real-time quantitative PCR analysis.

Gene [1]	GenBank Number	Primer Sequence (5′ to 3′)	Product Size
OTUD7A	XM_013177443.1	F: CAGACTTTGTTCGGTCCACA R: AGCAATGTCATCCTGCCTCT	236
MPAO	XM_013199765.1	F: TCCGACATGCAGTCCTTGTA R: AACCTTGTTGCCGTAGTTGG	201
IFIT5	XM_013194152.1	F: CCTTGAAGAAGTCCCTGCTG R: ATTTTCCAGGGCTTCCTTGT	194
IL23R	XM_013193090.1	F: CTGATGGGCTCCAACATCTC R: CTGTAGGGCAGCCTGAAGTC	161
TNFSF8	XM_013182840.1	F: AGGCTTGGAGCCACTAACAA R: GGTCGGGACATTCTGTAGGA	201
SAMD9	XM_013187038.1	F: CTCTCGCACAAATGGCACTA R: AGCTTTTGCAGCTCCAATGT	157
RSAD2	XM_013172803.1	F: GAGAGCGGTGGTTCAAGAAG R: TTGAGTGCCATGATCTGCTC	238
MX1	XM_013181384.1	F: TGGAGCAAGTAAACGCCTCT R: TTCAGGCACTGGTAGGCTTT	216
GBP1	XM_013170751.1	F: GAGCAGGAGAGAGAGGCTGA R: TGTTCTTCTCGGAGCCACTT	190
GAPDH	XM_013199522.1	F: GCCATCAATGATCCCTTCAT R: CTGGGGTCACGCTCCTG	155

[1] *OTUD7A*: ovarian tumor deubiquitinase 7A; *MPAO*: membrane primary amine oxidase; *IFIT5*: interferon-induced protein with tetratricopeptide repeats 5; *IL23R*: interleukin-23 receptor; *TNFSF8*: tumor necrosis factor ligand superfamily member 8; *SAMD9*: sterile alpha motif domain-containing protein 9; *RSAD2*: radical *S*-adenosyl methionine domain-containing protein 2; *GBP1*: interferon-induced guanylate binding protein 1-like; *MX1*: interferon-induced GTP-binding protein Mx1.

2.7. Statistical Analysis

The data were confirmed for normal distribution using the Shapiro–Wilk test. Significance was determined using Student's *t*-test for pairwise comparisons, and considered significant at $p < 0.05$.

3. Results

3.1. Genes and Pathways Affected by OTUD7A

RNA sequencing analysis of the transcriptomes of goose hepatocytes transfected with the *OTUD7A* overexpression vector vs. empty vector (as control) revealed 34 DEGs (19 upregulated and 15 downregulated) (Supplementary Figure S1). The upregulated and downregulated genes are shown in Tables 2 and 3, respectively. The enriched KEGG pathways were "cytokine–cytokine receptor interaction", "tropane, piperidine, and pyridine alkaloid biosynthesis", "isoquinoline alkaloid biosynthesis", "Janus kinase-signal transducer and activator of transcription (JAK-STAT) signaling pathway", and "PI3K-Akt signaling pathway" (Figure 1). RT-qPCR analysis of nine DEGs was performed to confirm the results of transcriptome analysis. Consistently, the expression of *OTUD7A*, membrane primary amine oxidase (*MPAO*), and interleukin-23 receptor (*IL23R*) was markedly induced by *OTUD7A* overexpression, whereas that of interferon-induced protein with tetratricopeptide repeats 5 (*IFIT5*), TNF ligand superfamily member 8 (*TNFSF8*), sterile alpha motif domain-containing protein 9 (*SAMD9*), radical *S*-adenosyl methionine domain-containing protein 2 (*RSAD2*), interferon-induced GTP-binding protein Mx1 (*MX1*), and interferon-induced guanylate binding protein 1-like (*GBP1*) was significantly inhibited ($p < 0.05$, Figure 2).

These findings were validated in a knockdown assay in goose primary hepatocytes with siRNA against goose *OTUD7A*. Compared with the controls, the mRNA expression of *MPAO*, *IFIT5*, *TNFSF8*, *SAMD9*, *RSAD2*, *MX1*, and *GBP1* was significantly increased by *OTUD7A* siRNA, whereas the *IL23R* expression was decreased ($p < 0.05$, Figure 3).

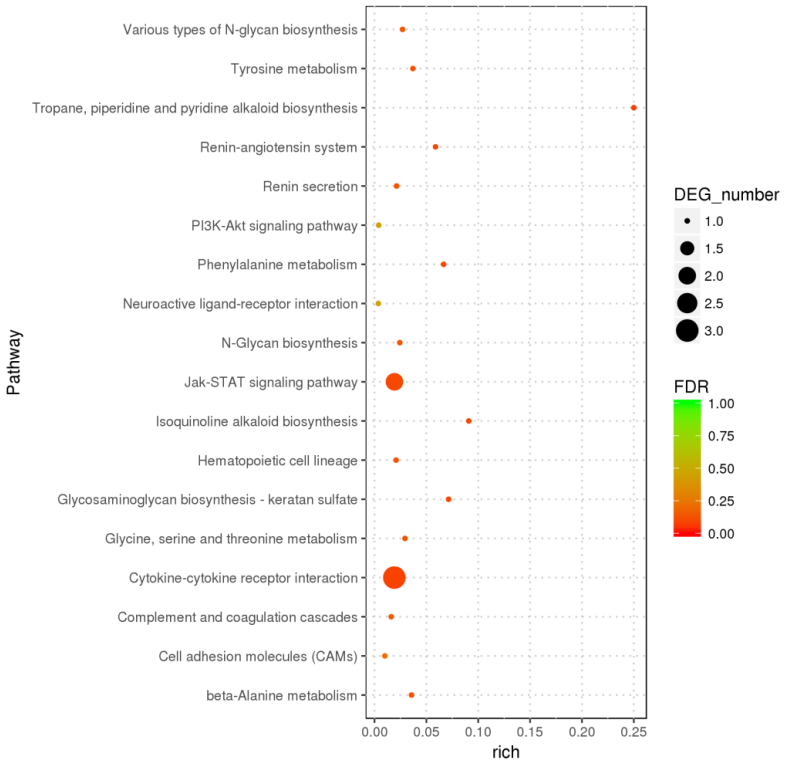

Figure 1. Kyoto Encyclopedia of Genes and Genomes (KEGG) analysis of the control and ovarian tumor deubiquitinase 7A (*OTUD7A*) overexpression groups in goose hepatocytes. Primary hepatocytes were isolated from goose embryos after 23 days of incubation. The cells transfected with the empty pcDNA3.1(+) vector were used as controls, while those transfected with pcDNA3.1(+) containing the *OTUD7A* coding sequence were used for overexpression. Differentially expressed genes (DEGs) were identified using DESeq2 R software. The DEGs were selected based on genes showing a fold change in *OTUD7A* overexpression compared to the control group of >2 or <0.5, and *p*-value < 0.05. The clusterProfiler R package was used to statistically analyze the enrichment of the DEGs in the KEGG pathways.

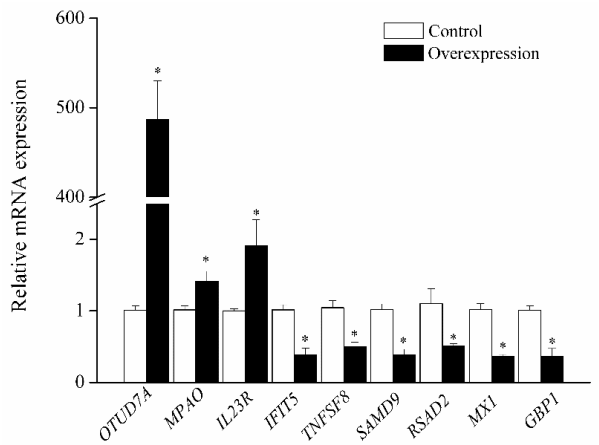

Figure 2. Validation of differentially expressed genes of the control and ovarian tumor deubiquitinase 7A (*OTUD7A*) overexpression groups in goose hepatocytes; * $p < 0.05$. Data are shown as the mean ± SEM of six replicates for each treatment. *MPAO*: membrane primary amine oxidase; *MX1*: interferon-induced GTP-binding protein Mx1; *IL23R*: interleukin-23 receptor; *IFIT5*: interferon-induced protein with tetratricopeptide repeats 5; *TNFSF8*: tumor necrosis factor ligand superfamily member 8; *RSAD2*: radical *S*-adenosyl methionine domain-containing protein 2; *GBP1*: interferon-induced guanylate binding protein 1-like; *SAMD9*: sterile alpha motif domain-containing protein 9.

Table 2. The upregulated genes in hepatocytes transfected with pcDNA3.1(+) containing goose OTU deubiquitinase 7A CDS and an empty vector.

Name	Description	*p*-Value	Fold Change
SNCG	Gamma-synuclein isoform	0.019	2.11
GPRIN2	G protein-regulated inducer of neurite outgrowth 2 isoform	0.039	2.29
NMU	Neuromedin-U isoform	0.004	7.86
OTUD7A	OTU domain-containing protein 7A	<0.001	134.69
LOC106034831	CMRF35-like molecule 3 isoform	0.018	4.68
ARHGAP28	Rho GTPase-activating protein 28 isoform	0.040	2.10
SH3BP1	SH3 domain-binding protein 1	0.040	2.82
MEST	Mesoderm-specific transcript homolog protein, partial	0.045	2.75
PROCR	Endothelial protein C receptor	0.004	2.61
CLMP	CXADR-like membrane protein	0.012	2.40
KLHDC8A	Kelch domain-containing protein 8A	0.047	3.32
MYL10	Myosin regulatory light chain 2B, cardiac muscle isoform	0.019	2.07
IL23R	Interleukin-23 receptor	0.017	2.14
LOC106045877	Alpha-1,3-mannosyl-glycoprotein 4-beta-N-acetylglucosaminyltransferase C-like	0.042	2.06
ACE	Angiotensin-converting enzyme	0.002	2.05
TMEM114	Transmembrane protein 114	0.004	3.64
PPP1R27	Protein phosphatase 1 regulatory subunit 27	0.05	2.99
MPAO	Membrane primary amine oxidase	0.045	2.03
LOC106048707	Uncharacterized protein LOC106048707 isoform	0.045	4.52

Table 3. The downregulated genes in hepatocytes transfected with pcDNA3.1(+) containing goose OTU deubiquitinase 7A CDS and an empty vector.

Name	Description	*p*-Value	Fold Change
IFIT5	Interferon-induced protein with tetratricopeptide repeats 5	<0.001	0.42
OTOGL	Otogelin-like protein	0.045	0.45
LOC106030637	Interleukin-7-like	0.022	0.17
RSAD2	Radical S-adenosyl methionine domain-containing protein 2	<0.001	0.48
DDX60	Probable ATP-dependent RNA helicase DDX60 isoform	<0.001	0.42
MX1	Interferon-induced GTP-binding protein Mx1	<0.001	0.47
NCAM2	Neural cell adhesion molecule 2 isoform	0.007	0.27
TNFSF8	Tumor necrosis factor ligand superfamily member 8	0.041	0.35
PIH1D3	Protein PIH1D3	0.035	0.39
LOC106038693	Low-affinity vacuolar monovalent cation antiporter	0.043	0.08
SAMD9	Sterile alpha motif domain-containing protein 9	<0.001	0.45
LOC106040189	Arylacetamide deacetylase-like 4	0.010	0.42
LOC106041938	Placenta-specific gene 8 protein-like isoform	<0.001	0.44
B3GNT7	UDP-GlcNAc:betaGal beta-1,3-N-acetylglucosaminyltransferase 7	<0.001	0.36
GBP1	Interferon-induced guanylate-binding protein 1	<0.001	0.45

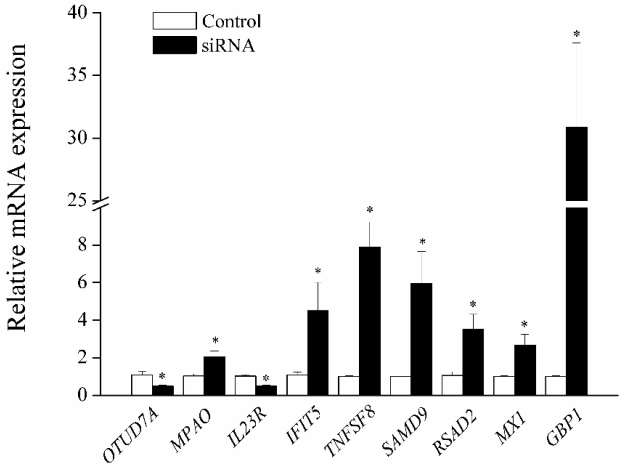

Figure 3. Effects of transfection with siRNA targeting ovarian tumor deubiquitinase 7A (*OTUD7A*) on the expression of downstream genes in goose primary hepatocytes. Scrambled siRNA was used as a control; * $p < 0.05$. Six replicates were evaluated for each treatment. Data are shown as the mean ± SEM.

3.2. Expression of OTUD7A and Its Downstream Genes

The expression of *OTUD7A*, *MPAO*, and *IL23R* was upregulated, whereas that of *IFIT5*, *TNFSF8*, *SAMD9*, *RSAD2*, *MX1*, and *GBP1* was downregulated at day 12 of overfeeding ($p < 0.05$, Figure 4A). However, the *OTUD7A* and *MPAO* expression was downregulated in goose fatty liver, whereas that of *IL23R*, *IFIT5*, *SAMD9*, *MX1*, and *GBP1* was upregulated on day 24 of overfeeding ($p < 0.05$, Figure 4B).

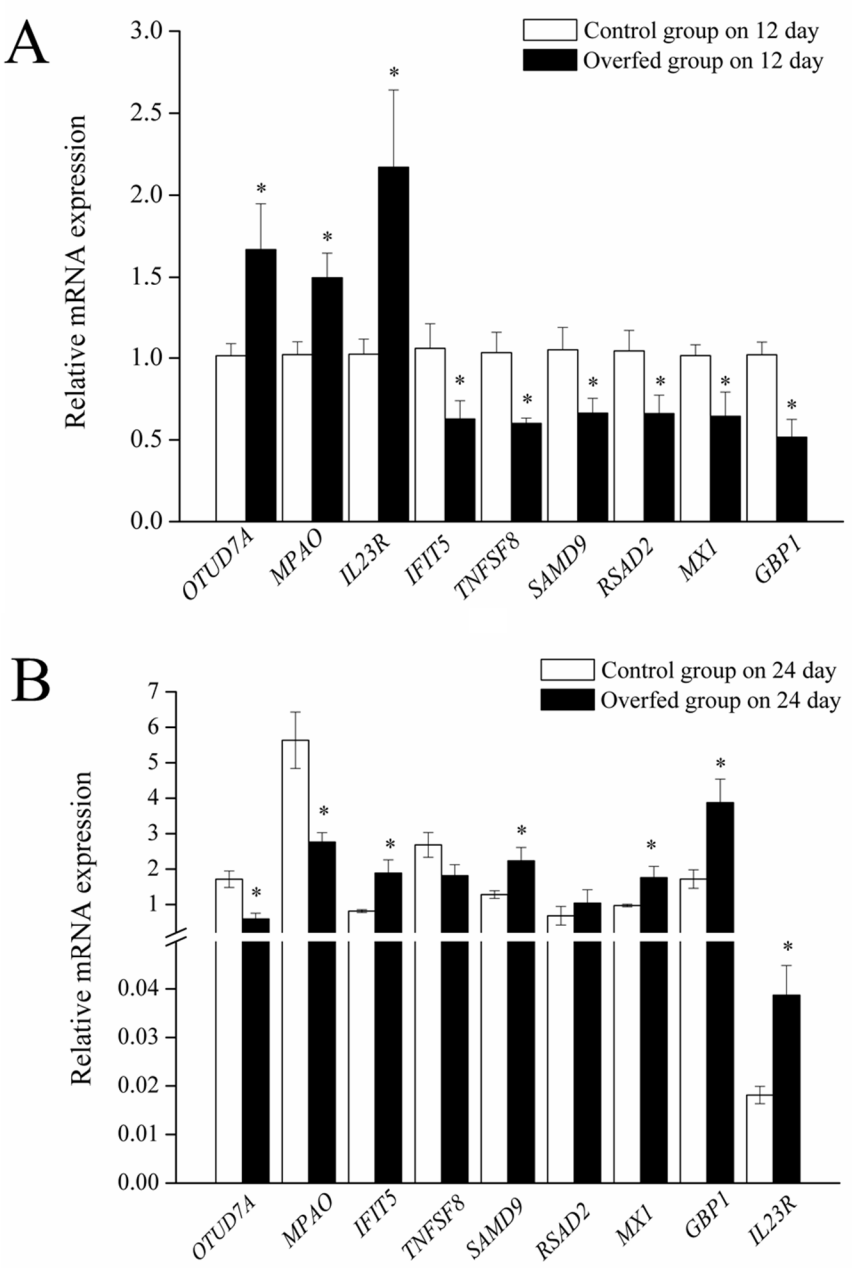

Figure 4. Effects of overfeeding on expression of downstream genes. Control group denotes geese that were fed normally; overfed group denotes geese subjected to 12 (**A**) and 24 days (**B**) of overfeeding; * $p < 0.05$. Samples in the control group on day 12 of overfeeding were used as calibrators for all groups. Six replicates were evaluated for each treatment. Data are shown as the mean ± SEM.

4. Discussion

The pathogenesis of NAFLD is still unclear. Previous studies have indicated that inflammatory responses play important roles in NAFLD, and inflammation is considered to be a marker of progression from simple steatosis to NASH [5,16,17]. Inflammation not only

aggravates insulin resistance, but also causes hepatic stellate cell activation, and induces liver fibrosis and cirrhosis [10,18]. The NF-κB pathway—a major inflammatory signaling pathway—is activated in patients with NAFLD and in animal models [5,6]. Activation of the NF-κB pathway can promote transcription of downstream inflammatory response genes, resulting in an increase in inflammatory factor production and release. Inflammatory factors can successively reactivate NF-κB, creating positive feedback regulation that leads to further amplification of the initial inflammatory signal [19]. In addition, NF-κB activation can activate pro-apoptotic proteins on mitochondria, such as BAX, leading to apoptosis of hepatocytes and further exacerbating the inflammatory response [20]. Reducing inflammatory factor expression in the liver can alleviate NAFLD development [11]; therefore, inflammation has received considerable attention as a possible target for NAFLD therapy.

As an excellent waterfowl product, goose fatty liver can be used as both a high-grade food and a unique model for NAFLD research. Our preliminary research has identified some characteristics that are different from mammalian NAFLD, such as elevated fatty acid desaturase, increased expression of lipocalin receptor genes, increased expression of mitochondria-related genes, and downregulated expression of complement genes and pro-inflammatory factors in goose fatty liver [2–4,21]. These results suggest the existence of certain mechanisms in the formation of goose fatty liver that can resist the occurrence and development of inflammation. Some studies suggest that deubiquitinating enzymes are involved in protecting against inflammation in NAFLD. Ubiquitin-specific protease 18—a member of the deubiquitinating enzyme family—is downregulated in the livers of obese mice [22]. Similarly, USP4 protects against the inflammatory response, as USP4 depletion was shown to exacerbate inflammation in mice with high-fat-diet-induced NAFLD, and USP4 may suppress activation of the downstream NF-κB pathway [23]. Mevissen et al. [12] found that *OTUD7A* is a potential tumor suppressor, and can regulate multiple signaling pathways. Another study indicated that *OTUD7A* inhibits the NF-κB pathway through deubiquitination of TRAF6 protein in HepG2 cells [10]. Therefore, *OTUD7A* may be involved in the development of fatty liver.

In this study, transcriptome sequencing analysis showed that a total of 19 genes were upregulated and 15 genes were downregulated in the *OTUD7A* overexpression group compared to controls. The DEGs were mainly enriched in cytokine–cytokine receptor interaction; tropane, piperidine, and pyridine alkaloid biosynthesis; isoquinoline alkaloid biosynthesis, the JAK-STAT signaling pathway; and the PI3K-Akt signaling pathway. Further analysis showed that numerous DEGs affected by *OTUD7A* were related to inflammation, as their mRNA expression was subject to *OTUD7A* overexpression or suppression by siRNA against *OTUD7A*, which is similar to the *OTUD7A* subfamily that can regulate some inflammation-related genes [24,25]. Our findings also support the hypothesis that OTUD7A can regulate the NF-κB pathway via deubiquitination of TRAF6. Pro-inflammatory factors can activate the inflammatory cascade response and increase the expression of genes such as *IL-6* and inducible nitric oxide synthase, causing inflammatory responses and tissue damage in the body. During the formation of mammalian NAFLD, the levels of pro-inflammatory factors are usually significantly elevated [18,26]. These results suggest that *OTUD7A* may be associated with the inhibition of inflammatory responses in goose fatty liver—at least in the mid-overfeeding period.

Interestingly, cytokine–cytokine receptor interactions, which are important for the maintenance and regulatory functions of multicellular organisms [27], were among the enriched KEGG pathways in the *OTUD7A* assay. Tumor necrosis factor superfamily (TNFSF) is a cytokine secreted by immune cells. The interaction between TNFSF and tumor necrosis factor receptor is involved in regulating cell growth, immune response, apoptosis, and inflammatory response [28]. The TNFSF8 protein can activate the NF-κB pathway by binding to its receptor, TNFRSF8, thereby mediating the secretion of IL-2, IL-6, TNF-α, and other cytokines [29]. The expression of *TNFSF8* was downregulated by *OTUD7A* overexpression in primary goose hepatocytes, as well as in goose fatty liver after 12 days of overfeeding, whereas the expression of *TNFSF8* was increased after *OTUD7A* suppression

in primary goose hepatocytes, suggesting that *TNFSF8* is regulated by *OTUD7A* in goose hepatocytes through the cytokine receptor interaction pathway.

The JAK-STAT pathway, as a downstream pathway of cytokine receptors, was also enriched according to the transcriptomic analysis of goose primary hepatocytes overexpressing *OTUD7A*. Several cytokines, including interferons, can modulate intracellular signaling by activating the JAK-STAT pathway [30]. Upon the binding of cytokines to their cognate receptors, STATs can modulate the expression of their target genes and participate in inflammation [31,32]. Enrichment of DEGs in the JAK-STAT signaling pathway resulting from *OTUD7A* overexpression suggests that *OTUD7A* regulates inflammation through the JAK-STAT signaling pathway in goose hepatocytes. The IFIT family, as interferon-induced genes, participate in the immune response [33]. Previous studies indicated that *IFIT5* promotes NF-κB activation and synergizes NF-κB-mediated gene expression, whereas knockdown of *IFIT5* inhibits NF-κB pathway activation and downstream gene expression [34,35]. Our data indicate that *IFIT5* expression was significantly decreased by *OTUD7A* overexpression, but was induced by *OTUD7A* knockdown in primary goose hepatocytes. Downregulation of *IFIT5* was accompanied by upregulation of *OTUD7A* on day 12 of overfeeding, whereas upregulation of *IFIT5* was accompanied by downregulation of *OTUD7A* on day 24 of overfeeding, which is consistent with the results of the cell research. Thus, *OTUD7A* may regulate *IFIT5* expression in the goose fatty liver. In addition, previous studies have suggested that *SAMD9* is a downstream target of inflammatory cytokines [36,37], and may function as an anti-inflammatory factor [38]; it is also associated with the immune response [39]. Our data indicate that *SAMD9*, like *IFIT5*, is regulated by *OTUD7A*.

Moreover, many studies have indicated that innate immune response is connected with inflammation in NAFLD/NASH, thereby promoting the development of fibrosis, cirrhosis, and carcinogenesis. The results from our study showed that *OTUD7A* regulates the expression of some immune-related genes—for example, *IL23R*—in goose fatty liver. *IL23R* mediates the stimulation of T cells, natural killer cells, and possibly certain macrophage/myeloid cells—likely through the JAK-STAT pathway [40]. In addition, the mRNA expression of *RSAD2*, *MX1*, and *GBP1* was downregulated by *OTUD7A* overexpression, but upregulated by *OTUD7A* knockdown. These results suggest that *RSAD2*, *MX1*, and *GBP1* are downstream of *OTUD7A*. *RSAD2*, also known as viperin, is an important component of innate immunity [41]. MX1 is also a vital antiviral protein during the innate immune response [42,43]. Some studies have shown that *GBP1* can be induced by IFN-α, IFN-β, IFN-γ, and inflammatory cytokines [44,45]. *GBP1* expression is increased in inflammatory skin diseases, and the gene is a cellular activation marker characterizing the inflammatory cytokine-activated phenotype of cells [46]. As immune-related genes, *IL23R*, *RSAD2*, *MX1*, and *GBP1* were regulated by *OTUD7A*, suggesting that *OTUD7A* can regulate immune response in liver physiology and pathology.

Additionally, KEGG results suggested that the DEGs were related to tropane, piperidine, pyridine, and isoquinoline alkaloid biosynthesis following *OTUD7A* overexpression; for example, *MPAO*, which participates in the metabolism of alkaloid biosynthesis, was upregulated by *OTUD7A* overexpression in goose primary hepatocytes. Consistently, upregulation of *MPAO* was accompanied by upregulation of *OTUD7A* on day 12 of overfeeding, whereas the downregulation of *MPAO* was accompanied by downregulation of *OTUD7A* on day 24 of overfeeding. Therefore, *OTUD7A* may participate in alkaloid biosynthesis in the goose fatty liver. Bour et al. [47] found that *MPAO* expression was increased in the adipose tissue, suggesting that it is involved in adipogenesis. Fat metabolism is very active in the formation of goose fatty liver [3]; thus, *MPAO* may be involved in lipid metabolism in the goose fatty liver. Further research is required in order to confirm this hypothesis.

5. Conclusions

Transcriptome sequencing analysis showed that *OTUD7A* is involved in the development of goose fatty liver, mainly through cytokine–cytokine receptor interaction; tropane,

piperidine, and pyridine alkaloid biosynthesis; isoquinoline alkaloid bio-synthesis; the JAK-STAT signaling pathway, and the PI3K-Akt signaling pathway. In addition, *OTUD7A* may regulate the expression of inflammation- and immune-related genes such as *TNFSF8*, *IFIT5*, *IL23R*, *RSAD2*, *MX1*, and *GBP1* in the goose fatty liver.

Supplementary Materials: The following are available online at https://www.mdpi.com/article/10.3390/agriculture12010105/s1: Figure S1: Genes affected by OTU deubiquitinase 7A (*OTUD7A*) overexpression; Figure S2: Screening of small interfering RNAs (siRNAs) for OTU deubiquitinase 7A (*OTUD7A*).

Author Contributions: Conceptualization, T.G. and D.G.; methodology, K.W., D.J. and M.K.K.; software, M.Z.; validation, M.Z. and L.L.; formal analysis, M.Z. and X.F.; investigation, D.G.; resources, M.Z.; data curation, Q.S.; writing—original draft preparation, M.Z.; writing—review and editing, T.G., D.J. and M.K.K.; visualization, D.G.; supervision, D.G.; project administration, D.G.; funding acquisition, M.Z. and D.G. All authors have read and agreed to the published version of the manuscript.

Funding: This research was funded by the National Nature Science Foundation of China, grant numbers 31802052, 31972546, and 32072785; the China Postdoctoral Science Foundation (2017M621840); and the Priority Academic Program Development of Jiangsu Higher Education Institutions (PAPD).

Institutional Review Board Statement: This study was approved by the Institutional Ethics Committee of Yangzhou University (protocol code 202103309, 9 March 2021).

Data Availability Statement: The data presented in this study are available upon request from the corresponding author.

Conflicts of Interest: The authors declare no conflict of interest.

References

1. Hermier, D.; Rousselot-Pailley, D.; Peresson, R.; Sellier, N. Influence of orotic acid and estrogen on hepatic lipid storage and secretion in the goose susceptible to liver steatosis. *Biochim. Biophys. Acta* **1994**, *1211*, 97–106. [CrossRef]
2. Geng, T.Y.; Xia, L.L.; Li, F.Y.; Xia, J.; Zhang, Y.H.; Wang, Q.Q.; Yang, B.; Montgomery, S.; Cui, H.M.; Gong, D.Q. The role of endoplasmic reticulum stress and insulin resistance in the occurrence of goose fatty liver. *Biochem. Biophys. Res. Commun.* **2015**, *465*, 83–87. [CrossRef]
3. Geng, T.Y.; Yang, B.; Li, F.Y.; Xia, L.L.; Wang, Q.Q.; Zhao, X.; Gong, D.Q. Identification of protective components that prevent the exacerbation of goose fatty liver: Characterization, expression and regulation of adiponectin receptors. *Comp. Biochem. Physiol. B Biochem. Mol. Biol.* **2016**, *194–195*, 32–38. [CrossRef]
4. Liu, L.; Zhao, X.; Wang, Q.; Sun, X.X.; Xia, L.L.; Wang, Q.Q.; Yang, B.; Zhang, Y.H.; Montgomery, S.; Meng, H.; et al. Prosteatotic and protective components in a unique model of fatty liver: Gut microbiota and suppressed complement system. *Sci. Rep.* **2016**, *6*, 31763. [CrossRef]
5. Baker, R.G.; Hayden, M.S.; Ghosh, S. NF-κB, inflammation, and metabolic disease. *Cell Metab.* **2011**, *13*, 11–22. [CrossRef] [PubMed]
6. Zhou, Y.; Ding, Y.L.; Zhang, J.L.; Zhang, P.; Wang, J.Q.; Li, Z.H. Alpinetin improved high fat diet-induced non-alcoholic fatty liver disease (NAFLD) through improving oxidative stress, inflammatory response and lipid metabolism. *Biomed. Pharmacother.* **2018**, *97*, 1397–1408. [CrossRef]
7. Hossain, N.; Kanwar, P.; Mohanty, S.R. A comprehensive updated review of pharmaceutical and nonpharmaceutical treatment for NAFLD. Gastroenterol. *Res. Pract.* **2016**, *144*, 7109270.
8. Rahman, A.M.; Mahdavi, A.H.; Rahmani, H.R.; Jahanian, E. Clove bud (*Syzygium aromaticum*) improved blood and hepatic antioxidant indices in laying hens receiving low n-6 to n-3 ratios. *J. Anim. Physiol. Anim. Nutr.* **2017**, *101*, 881–892. [CrossRef] [PubMed]
9. Marra, F. Nuclear factor-κB inhibition and non-alcoholic steatohepatitis: Inflammation as a target for therapy. *Gut* **2008**, *57*, 570–572. [CrossRef] [PubMed]
10. Tilg, H.; Moschen, A.R. Evolution of inflammation in nonalcoholic fatty liver disease: The multiple parallel hits hypothesis. *Hepatology* **2010**, *52*, 1836–1846. [CrossRef] [PubMed]
11. Tian, Y.L.; Ma, J.T.; Wang, W.D.; Zhang, L.J.; Xu, J.; Wang, K.; Li, D.F. Resveratrol supplement inhibited the NF-κB inflammation pathway through activating AMPKα-SIRT1 pathway in mice with fatty liver. *Mol. Cell. Biochem.* **2016**, *422*, 75–84. [CrossRef]
12. Mevissen, T.E.; Hospenthal, M.K.; Geurink, P.P.; Elliott, P.R.; Akutsu, M.; Arnaudo, N.; Ekkebus, R.; Kulathu, Y.; Wauer, T.; Oualid, F.E.I.; et al. OTU deubiquitinases reveal mechanisms of linkage specificity and enable ubiquitin chain restriction analysis. *Cell* **2013**, *154*, 169–184. [CrossRef]
13. Xu, Z.; Pei, L.; Wang, L.; Zhang, F.; Hu, X.; Gui, Y. Snail1-dependent transcriptional repression of Cezanne2 in hepatocellular carcinoma. *Oncogene* **2014**, *33*, 2836–2845. [CrossRef]

14. Zhao, M.M.; Liu, T.J.; Wang, Q.; Zhang, R.; Liu, L.; Gong, D.Q.; Geng, T.Y. Fatty acids modulate the expression of pyruvate kinase and arachidonate-lipoxygenase through PPARγ/CYP2C45 pathway: A link to goose fatty liver. *Poult. Sci.* **2019**, *98*, 4346–4358. [CrossRef] [PubMed]
15. Schmittgen, T.D.; Livak, K.J. Analyzing real-time PCR data by the comparative CT method. *Nat. Protoc.* **2008**, *3*, 1101–1108. [CrossRef] [PubMed]
16. Parola, M.; Vajro, P. Nocturnal hypoxia in obese-related obstructive sleep apnea as a putative trigger of oxidative stress in pediatric NAFLD progression. *J. Hepatol.* **2016**, *65*, 470–472. [CrossRef]
17. Wruck, W.; Graffmann, N.; Kawala, M.A.; Adjaye, J. Concise review: Current status and future directions on research related to nonalcoholic fatty liver disease. *Stem Cells* **2017**, *35*, 89–96. [CrossRef]
18. Pirozzi, C.; Lama, A.; Simeoli, R.; Paciello, O.; Pagano, T.B.; Mollica, M.P.; Di Guida, F.; Russo, R.; Magliocca, S.; Canani, R.B.; et al. Hydroxytyrosol prevents metabolic impairment reducing hepatic inflammation and restoring duodenal integrity in a rat model of NAFLD. *J. Nutr. Biochem.* **2016**, *30*, 108–115. [CrossRef] [PubMed]
19. Kondylis, V.; Kumari, S.; Vlantis, K.; Pasparakis, M. The interplay of IKK, NF-κB and RIPK1 signaling in the regulation of cell death, tissue homeostasis and inflammation. *Immunol. Rev.* **2017**, *277*, 113–127. [CrossRef]
20. John, J.L.; Qian, T.; He, L.H.; Kim, J.S.; Elmore, S.P.; Cascio, W.E.; Brenner, D.A. Role of mitochondrial inner membrane permeabilization in necrotic cell death, apoptosis, and autophagy. *Antioxid. Redox. Signal.* **2002**, *4*, 769–781.
21. Xing, Y.; Xu, C.; Lin, X.; Zhao, M.M.; Gong, D.Q.; Liu, L.; Geng, T.Y. Complement C3 participates in the development of goose fatty liver potentially by regulating the expression of FASN and ETNK1. *Anim. Sci. J.* **2021**, *92*, e13527. [CrossRef] [PubMed]
22. An, S.; Zhao, L.P.; Shen, L.J.; Wang, S.; Zhang, K.; Qi, Y.; Zheng, J.; Zhang, X.J.; Zhu, X.Y.; Bao, R.; et al. USP18 protects against hepatic steatosis and insulin resistance through its deubiquitinating activity. *Hepatology* **2017**, *666*, 1866–1884. [CrossRef]
23. Zhao, Y.C.; Wang, F.; Gao, L.C.; Xu, L.W.; Tong, R.Y.; Lin, N.; Su, Y.Y.; Yan, Y.; Gao, Y.; He, J.; et al. Ubiquitin-specific protease 4 is an endogenous negative regulator of metabolic dysfunctions in nonalcoholic fatty liver disease in mice. *Hepatology* **2018**, *68*, 897–917. [CrossRef] [PubMed]
24. Lin, D.D.; Shen, Y.; Qiao, S.; Liu, W.W.; Zheng, L.S.; Wang, Y.N.; Cui, N.P.; Wang, Y.F.; Zhao, S.L.; Shi, J.H. Upregulation of OTUD7B (cezanne) promotes tumor progression via AKT/VEGF pathway in lung squamous carcinoma and adenocarcinoma. *Front. Oncol.* **2019**, *9*, 862. [CrossRef]
25. Deng, J.J.; Hou, G.X.; Fang, Z.X.; Liu, J.L.; Lv, X.D. Distinct expression and prognostic value of OTU domain-containing proteins in non-small-cell lung cancer. *Oncol. Lett.* **2019**, *5*, 5417–5427. [CrossRef] [PubMed]
26. Ceccarelli, S.; Panera, N.; Mina, M.; Gnani, D.; Stefanis, C.D.; Crudele, A.; Rychlicki, C.; Petrini, S.; Bruscalupi, G.; Agostinelli, L.; et al. LPS-induced TNF-α factor mediates pro-inflammatory and pro-fibrogenic pattern in non-alcoholic fatty liver disease. *Oncotarget* **2015**, *6*, 41434–41452. [CrossRef] [PubMed]
27. Leonard, W.J.; Lin, J.X. Cytokine receptor signaling pathways. *J. Allergy Clin. Immunol.* **2000**, *105*, 877–888. [CrossRef]
28. Croft, M.; Duan, W.; Choi, H.; Eun, S.Y.; Madireddi, S.; Mehta, A. TNF superfamily in inflammatory disease: Translating basic insights. *Trends Immunol.* **2012**, *33*, 144–152. [CrossRef] [PubMed]
29. Horie, R.; Aizawa, S.; Nagai, M.; Ito, K.; Higashihara, M.; Ishida, T.; Inoue, J.; Watanabe, T. A novel domain in the CD30 cytoplasmic tail mediates NFkappaB activation. *Int. Immunol.* **1998**, *10*, 203–210. [CrossRef]
30. McGillicuddy, F.C.; Chiquoine, E.H.; Hinkle, C.C.; Kim, R.J.; Shah, R.; Roche, H.M.; Smyth, E.M.; Reilly, M.P. Interferon γ attenuates insulin signaling, lipid storage, and differentiation in human adipocytes via activation of the JAK/STAT pathway. *J. Biol. Chem.* **2009**, *284*, 31936–31944. [CrossRef]
31. Imada, K.; Leonard, W.J. The Jak-STAT pathway. *Mol. Immunol.* **2000**, *37*, 1–11. [CrossRef]
32. Coskun, M.; Salem, M.; Pedersen, J.; Nielsen, O.H. Involvement of JAK/STAT signaling in the pathogenesis of inflammatory bowel disease. *Pharmacol. Res.* **2013**, *76*, 1–8. [CrossRef] [PubMed]
33. Rohaim, M.A.; Santhakumar, D.; Naggar, R.F.E.; Iqbal, M.; Hussein, H.A.; Munir, M. Chickens expressing IFIT5 ameliorate clinical outcome and pathology of highly pathogenic avian influenza and velogenic newcastle disease viruses. *Front. Immunol.* **2018**, *9*, 2025. [CrossRef] [PubMed]
34. Zhang, B.H.; Liu, X.Y.; Chen, W.; Chen, L. IFIT5 potentiates anti-viral response through enhancing innate immune signaling pathways. *Acta Biochim. Biophys. Sin.* **2013**, *45*, 867–874. [CrossRef]
35. Zheng, C.S.; Zheng, Z.H.; Zhang, Z.H.; Meng, J.; Liu, Y.; Ke, X.L.; Hu, Q.X.; Wang, H.Z. IFIT5 positively regulates NF-κB signaling through synergizing the recruitment of IκB kinase (IKK) to TGF-β-activated kinase 1 (TAK1). *Cell. Signal.* **2015**, *27*, 2343–2354. [CrossRef]
36. Chefetz, I.; Ben, A.D.; Browning, S.; Skorecki, K.; Adir, N.; Thomas, M.G.; Kogleck, L.; Topaz, O.; Indelman, M.; Uitto, J.; et al. Normophosphatemic familial tumoral calcinosis is caused by deleterious mutations in SAMD9, encoding a TNF-α responsive protein. *J. Investig. Dermatol.* **2008**, *128*, 1423–1429. [CrossRef]
37. Hershkovitz, D.; Gross, Y.; Nahum, S.; Yehezkel, S.; Sarig, O.; Uitto, J.; Sprecher, E. Functional characterization of SAMD9, a protein deficient in normophosphatemic familial tumoral calcinosis. *J. Investig. Dermatol.* **2011**, *131*, 662–669. [CrossRef]
38. He, P.; Wu, L.-F.; Bing, P.-F.; Xia, W.; Wang, L.; Xie, F.-F.; Lu, X.; Lei, S.-F.; Deng, F.-Y. SAMD9 is a (epi-) genetically regulated anti-inflammatory factor activated in RA patients. *Mol. Cell Biochem.* **2019**, *456*, 135–144. [CrossRef]
39. Nounamo, B.; Li, Y.B.; Byrne, P.O.; Kearney, A.M.; Khan, A.; Liu, J. An interaction domain in human SAMD9 is essential for myxoma virus host-range determinant M062 antagonism of host anti-viral function. *Virology* **2017**, *503*, 94–102. [CrossRef]

40. Parham, C.; Chirica, M.; Timans, J.; Vaisberg, E.; Travis, M.; Cheung, J.; Pflanz, S.; Zhang, R.; Singh, K.P.; Vega, F.; et al. A receptor for the heterodimeric cytokine IL-23 is composed of IL-12Rβ1 and a novel cytokine receptor subunit, IL-23R. *J. Immunol.* **2002**, *168*, 5699–5708. [CrossRef]
41. Rivieccio, M.A.; Suh, H.S.; Zhao, Y.M.; Zhao, M.L.; Chin, K.C.; Lee, S.C.; Brosnan, C.F. TLR3 ligation activates an antiviral response in human fetal astrocytes: A role for viperin/cig5. *J. Immunol.* **2006**, *177*, 4735–4741. [CrossRef] [PubMed]
42. Wisskirchen, C.; Ludersdorfer, T.H.; Müller, D.A.; Moritz, E.; Pavlovic, J. Interferon-induced antiviral protein MxA interacts with the cellular RNA helicases UAP56 and URH49. *J. Biol. Chem.* **2011**, *286*, 34743–34751. [CrossRef] [PubMed]
43. Xiao, J.; Yan, J.; Chen, H.; Li, J.; Tian, Y.; Tang, L.S.; Feng, H. Mx1 of black carp functions importantly in the antiviral innate immune response. *Fish Shellfish Immunol.* **2016**, *58*, 584–592. [CrossRef]
44. Tripal, P.; Bauer, M.; Naschberger, E.; Mörtinger, T.; Hohenadl, C.; Cornali, E.; Thurau, M.; Stürzl, M. Unique features of different members of the human guanylate-binding protein family. *J. Interferon Cytokine Res.* **2007**, *27*, 44–52. [CrossRef]
45. Britzen-Laurent, N.; Bauer, M.; Berton, V.; Fischer, N.; Syguda, A.; Reipschläger, S.; Naschberger, E.; Herrmann, C.; Stürzl, M. Intracellular trafficking of guanylate-binding proteins is regulated by heterodimerization in a hierarchical manner. *PLoS ONE* **2010**, *12*, e14246. [CrossRef] [PubMed]
46. Lubeseder-Martellato, C.; Guenzi, E.; Jörg, A.; Töpolt, K.; Naschberger, E.; Kremmer, E.; Zietz, C.; Tschachler, E.; Hutzler, P.; Schwemmle, M.; et al. Guanylate-binding protein-1 expression is selectively induced by inflammatory cytokines and is an activation marker of endothelial cells during inflammatory diseases. *Am. J. Pathol.* **2002**, *161*, 1749–1759. [CrossRef]
47. Bour, S.; Daviaud, D.; Gres, S.; Lefort, C.; Prévot, D.; Zorzano, A.; Wabitsch, M.; Saulnier-Blache, J.-S.; Valet, P.; Carpéné, C. Adipogenesis-related increase of semicarbazide-sensitive amine oxidase and monoamine oxidase in human adipocytes. *Biochimie* **2007**, *89*, 916–925. [CrossRef] [PubMed]